High CRMP2 expression in peripheral T lymphocytes is associated with recruitment to the brain during virus-induced neuroinflammation.

C. Vuaillat, M. Varrin-Doyer, A. Bernard, I. Sagardoy, S. Cavagna, I. Chounlamountri, M. Lafon, P. Giraudon

High CRMP2 expression in peripheral T lymphocytes is associated with recruitment to the brain during virus-induced neuroinflammation

Vuaillat C, Varrin-Doyer M, Bernard A, Sagardoy I, Cavagna S, N Chounlamountri, IA, Lafon M [*], Giraudon P

Inserm, U842, Lyon, F-69372; Inserm, IFR19, Bron, F-69677 France; Université de Lyon, Lyon, F-69000 France

[*] Institut Pasteur, Viral Neuroimmunology, Paris, F-75015 France

Corresponding author: Pascale Giraudon, U842 Inserm, Rue Guillaume Paradin, Faculté de Médecine Laënnec, F-69372 Lyon, Cedex, France

giraudon@lyon.inserm.fr; Fax 33 4 78 77 86 16

Funds: ARSEP, Internal grants from Institut Pasteur (ML) and INSERM

Abstract

Collapsin Response Mediator Protein (CRMP)-2 is involved in T-cell polarization and migration. To address the role of CRMP2 in neuroinflammation, we analyzed its involvement in lymphocyte recruitment to the central nervous system in mouse infected with neurotropic and non-neurotropic virus strains (RABV, CDV). A sub-population of early-activated CD69+CD3+ T lymphocytes highly expressing CRMP2 (CRMP2hi) peaked in the blood, lymph nodes and brain of mice infected with neurotropic viruses, and correlated with severity of disease. They displayed high migratory properties reduced by CRMP2 blocking antibody. These data point out the potential use of CRMP2 as a peripheral indicator of neuroinflammation.

Key words: neuroimmunology, neurovirology, neuroinflammatory disease, T-cell motility, rabies virus, canine distemper virus

1- **Introduction**

In acute viral encephalitis, the recruitment of immune cells to the central nervous system (CNS) plays a crucial role in the outcome of this disease. Notably, T-lymphocytes are key players in the initiation of specific intrathecal immune responses by directly destroying virus-infected cells, increasing the phagocytotic activity of macrophages and stimulating the production of antibodies by B cells (Fujinami et al., 2006; Salazar-Mather and Hokeness, 2006; Tishon et al., 2006). Thus, immune cells control the spread of viruses and participate in viral clearance. However, T-lymphocytes can mediate inappropriate inflammatory responses, producing multiple cytokines, chemokines, and reactive oxygen species that contribute to severe neural tissue injury and CNS dysfunction (Carlson et al., 2006) (Peterson and Fujinami, 2007; Galelli et al., 2000; Giraudon et al., 2004; Lane et al., 2000; Patterson et al., 2003). Considering the importance of viral encephalitis in humans, the homing behavior and functional status of immune cells that infiltrate the virus-infected brain need to be clarified. Characterizing the mechanisms that favor the migration of T-lymphocytes to the CNS in response to viral infection is of interest both for understanding the physiopathology of virus-induced neuroinflammation and to propose new therapeutic approaches.

T-lymphocytes constantly move in and out of lymph nodes, circulating through the vasculature. Probably following activation and as a result of chemotactic stimuli, T-cells acquire a polarized morphology, leave the vasculature and start to crawl within neural tissue (Norman and Hickey, 2005; Sanchez-Madrid and del Pozo, 1999; Westermann et al., 2005). Dynamic cytoskeletal remodeling is fundamental to drive the rapid conversion of lymphocyte cytoarchitecture from a semi-rigid to a highly deformable state needed for transendothelial migration and crawling within CNS parenchyma (Vicente-Manzanares and Sanchez-Madrid, 2004). Thus, motile T-cells display a polarized morphology, with two distinct T-cell compartments. At the advancing front, the leading edge is enriched in chemokine receptors and acts as a sensor to the microenvironment. At the trailing edge, the uropod is an adhesive and retractile structure required for T-cell migration (Barreiro et al., 2004). Rapid reorganization of actin at the leading edge and the retraction of microtubule and vimentin networks in the uropod during polarization and migration have been well described (Brown et al., 2001; Mitchison and Cramer, 1996). Such a cytoskeletal reconfiguration requires a complex and still not completely defined array of intracellular signaling pathways implicating second messengers, several kinases and Rho family small GTPases (del Pozo et al., 1999; Vicente-Manzanares et al.,

2002). In search of molecules involved in cell motility and shared by the immune and nervous systems, we recently identified Collapsin Response Mediator Protein-2 (CRMP2) in T-lymphocytes (Vincent et al., 2005), a phosphoprotein described in neuron growth cone advance (Goshima et al, 1995) and neural cell migration via microtubule organization. We showed that CRMP2 redistributes in the uropod in motile T-cells, binds cytoskeletal elements and is implicated in T-cell polarization and migration (Vincent et al., 2005). A correlation between CRMP2 expression levels and cell migratory rates was demonstrated by over-expression and knock-down experiments in primary T-lymphocytes. The importance of CRMP2 in the immune response was emphasized by the observation that, in humans suffering from virus-induced neuroinflammatory disease, peripheral activated immune cells displayed high migratory rates associated with elevated CRMP2 expression (Vincent et al., 2005). These observations led us to suspect a role for CRMP2 in immune cell trafficking and recruitment to the inflamed CNS. In the present study, we evaluated the CRMP2 contribution in brain lymphocyte recruitment by analyzing CRMP2 expression in peripheral and brain-infiltrating immune cells in mouse models of infection using neurovirulent and non-neurovirulent strains of rabies virus (RABV) and Canine distemper virus (CDV). After inoculation of the neurovirulent RABV strain Challenge virus standard (CVS) in the muscle of the hind limb- to mimic the inoculation of this virus by an animal bite- the virus enters nerve endings via the neuromuscular junction and then travels from one neuron to another along the spinal cord before reaching the entire brain, causing severe neuronal dysfunctions and fatal encephalitis (Lafon, 2004). Infection in the CNS triggers a strong innate immune response in both neurons and astrocytes, resulting in inflammatory and chemo-attractive responses characterized by IFN–β, IL-1, IL6, TNF–α, CCL5, CXCL-10 expression capable of attracting T cells, B cells and macrophages through the blood brain barrier (Camelo et al., 2001a; Baloul et al., 2004; Wang et al., 2005; Roy et al., 2007). Inoculation of the Pasteur Virus (PV) RABV strain another neurovirulent RAV strain causes only spinal cord and the bulb infection, resulting in abortive rabies: mice cleared the CNS infection and survive despite paralytic sequel (6). By contrast, injection by the same route of the non-neuronotropic vaccine RABV strain ERA does not cause infection of the CNS and animals remain healthy. In the mouse model infected with CDV, intracerebral inoculation of a neurovirulent strain results in acute encephalitis followed, in surviving animals, by the development of motor impairment and metabolic disease (Bernard et al., 1999; Griffond et al., 2004; Verlaeten et al., 2001). CDV infects the neurons of defined brain structures (Bernard et al., 1993) and provokes a brain inflammatory

reaction with the infiltration of T lymphocytes, the expression of the cytokines TNFα, IL6, IFNγ and IL-4 associated with the disruption of the tissue inhibitor of the metalloprotease TIMP/ metalloprotease MMP balance (Benscsik et al., 1996; Khuth et al., 2001) capable of modifying vascular permeability.

We show here that, in contrast of what was observed in mice infected with non-neurovirulent virus strain, infection of the CNS with neuronotropic CDV and RABV enhanced both CRMP2 expression and migratory rate of activated T lymphocytes. Interestingly, the presence in blood and lymph nodes of lymphocytes expressing high CRMP2 level was associated with the intensity of recruitment of immune cells into the brain of mice suffering from encephalitis and correlated with the severity of clinical score.

2- **Material and Methods**

-Animal models

Mice, rabies infection and assessment of clinical symptoms

Experiments were performed with 6-week-old female BALB/c mice from Janvier (St. Berthevin, France). Mice were inoculated intramuscularly in both hind legs, with $1x10^7$ infectious RABV particles of different strains: Challenge Virus Standard, CVS-11, ADCC 959; ERA strain ADCC 332 (American Type Cell Collection, ADCC, Rockville); Pasteur virus strain (PV). Disease progression was evaluated by scoring mobility and mortality as follows: 0=normal mice, 1=ruffled fur, 2=loss of agility, 3=one paralyzed hind leg, 4=two paralyzed hind legs, 5=total loss of mobility and 6=death. Clinical signs were expressed as individual clinical sign values or as cumulative clinical signs by adding the individual clinical signs of the group. At various times after infection, blood was taken from the retro-orbital plexus and groups of two or three mice were perfused by intracardiac injection of 50 ml 0.1M phosphate buffer pH 7.4. Spleen, lymph nodes, spinal cords and brains were removed and processed to isolate mononuclear cells (8 infected mice and 8 controls analyzed). The presence of virus in the brain was checked during the experiments (not shown).

Mice, CDV infection and clinical symptoms

Four-week-old female outbred SV129 mice (Harlan-France) were inoculated intracerebrally (10μl) as already reported (Bernard et al., 1983) with a neonatal mouse brain suspension containing 200 to 1000 PFU of the mice neuroadapted Onderstepoort CDV strain shown to be neuronotropic. Control (sham-inoculated) mice were inoculated with brain homogenate from non-infected neonatal mice. Concomitant with active virus replication in selective brain structures, acute meningoencephalitis occurred in all mice and peaked on day 14 post-inoculation. At various times after virus inoculation, cardiac perfusion was performed and blood, spleen, lymph nodes, spinal cords and brains were removed and processed to isolate mononuclear cells on day 3 (n=3), day 7 (n=12), day 11 (n=5) and day 14 (n=8) as described above (3 different experiments). The presence of virus in the infected brain was checked during the experiments (not shown). Mice were housed in A2 animal colonies according to European Economic Community (86/609/EEC) and French (Decree 87-848) animal care regulations, in a temperature- and light-controlled room.

- Cell preparation

For peripheral blood mononuclear cell (PBMC) analysis**,** blood was collected at the retro-orbital plexus. PBMCs were then isolated on Ficoll-Hypaque (Eurobio), washed three times with PBS and re-suspended in PBS/2%FCS before immunocytochemistry and flow cytometry analysis. For lymph node mononuclear cell analysis, mononuclear cells were collected from popliteal (for RABV model) or cervical lymph nodes (for CDV model), following dissociation with a syringe plunger. Lymphocyte enrichment was performed by a 30 min contact of the cell preparation on a plastic dish to remove adherent phagocytes. Mononuclear cells infiltrating the CNS were collected using Percoll (Amersham Biosciences) gradients, as previously described (Camelo et al., 2001b).

- Flow cytometry phenotyping

Mononuclear cells were washed in PBS and then incubated for 15 min at room temperature (RT) with various combinations of fluorescence-conjugated mAbs (all from Beckman Coulter, unless otherwise specified) as follows: phycoerythrin (PE)-labeled anti-CD3, PE-labeled anti-CD69 and PE-labeled anti-CD11c. The stained cells were washed and fixed with 4% paraformaldehyde (PFA- Sigma) in PBS (pH 7.4) for 30 min at 4°C and washed again. Cells were then re-suspended in PBS at 4°C awaiting analysis (if surface staining alone was required) or processed further for intracellular CRMP2 protein detection. For the latter, cells were re-suspended in PBS containing 0.5% saponin (permeabilization buffer -PB) and incubated for 30 min at RT with rabbit anti-peptide4/CRMP2 antibody, prepared against a CRMP2 (Ricard et al., 2001). The cells were washed once with PBS 0.05% saponin and then incubated in PBS 0.5% saponin with fluorescein isothiocyanate (FITC)-labeled goat F(ab')2 anti-rabbit for 20 min at RT. Finally, the cells were washed with PBS 0.05% saponin, re-suspended in PBS, and analysed by flow cytometry on a Coulter EPICS XL (Beckman Coulter). Nonspecific staining was excluded by isotypic control gating.

- Immunohistochemistry

Analysis of infiltrating T cells was performed on brain slices using two different protocols of fixation. 1) For Diaminobenzidine staining, mice were perfused with PBS then PBS containing 1% PFA. Removed brains were then post-fixed in 1% PFA (1h, RT), immersed in 15% sucrose (overnight), frozen in isopentane cooled to -60°C and stored at -80°C until use. Coronal brain sections (cryo microtome, 14 to 20μm thick) from mice sacrificed on day 14 post-infection with CDV were collected on Superfrost

glass slides. Following treatment with reagent to eliminate nonspecific labeling due to endogenous biotin (Vector kit), slides were incubated for 24h with anti-mouse CD4 monoclonal antibody (clone H129.19, Pharmingen Int.). Samples were then sequentially washed and incubated with biotinylated anti-rabbit or anti-mice IgG antibodies (2h, RT), avidin-biotin peroxidase complex (VectaStain, 1h RT) and 3.3'-diaminobenzidine. 2) For immunofluorescence analysis, brain were removed and immediately frozen in isopentane cooled to -60°C and stored at -80°C until coronal sections and use. Fixation in absolute ethanol (10 min, RT) was required for CD4 and CD8 detection while acetone fixation (10 min, 4°C) was required for CRMP2 and TCR beta chain detection. Following 1h incubation with a blocking solution (PBS, 0,3% Triton, 1% BSA, 1% normal goat serum) to eliminate nonspecific labeling, slides were incubated with anti-mouse CD4 and CD8 (clone H129.19 and clone53-6.7, Pharmingen Int.) monoclonal antibodies or polyclonal anti-peptide4/CRMP2 antibody (Ricard et al., 2001). (2h, 37°C), then with anti-rat and anti-rabbit IgG Alexa 488 antibodies (2h, RT) (Molecular Probes, Inc.). T-cell receptor was detected using a FITC anti TCR beta chain (clone H57-597, BD Pharmingen). Omission of the primary or secondary antibody resulted in no signal.

- Transmigration assay

Transmigration of lymphocytes, isolated from lymph nodes as reported above, was performed both in micro-Transwell system as described (Vincent et al., 2005) and in organotypic culture of mice brain. For *ex vivo* transmigration on mice CNS, hippocampus cultures were prepared as follows. Hippocampi from postnatal (P7) C57BL6 mouse were dissected and placed immediately in cold Gey's balanced solution supplement with glucose (6,5mg/ml). Four hundred micrometer slices were cut perpendicularly to the septotemporal axis of the hippocampus using a McIllwain tissue chopper. Slices were carefully trimmed for excess tissue, and 6 slices were placed immediately on 30 mm semi-permeable membrane inserts (Millicell-CM, Millipore) in a 6-well plate containing 1 ml of culture medium in each well. The culture medium consisted of 50% Minimum Essential Medium (Gibco), 25% Hank's balanced salt solution, 25% heat-inactived horse serum (Gibco), 1% L-glutamine 200Mm (Gibco) and 6,5 mg/ml D-glucose. Plates were incubated at 37°C and 5% CO2. The culture medium was exchanged twice a week. Lymphocytes (1.10^6 cells per slice) stained ex vivo using the vital fluorochrome carboxyfluoroscein succinimidyl ester/CFSE (1mM, 5 min, 37°C) were spotted closely to hippocampus slices. Following a 18h contact at 37°C, slices were extensively washed with D-MEM,

fixed with ethanol (10 min, 4°C), incubated with 4', 6'-diamidino2-phenylindol/DAPI for nucleus staining. Numbers of infiltrating lymphocytes were counted under fluorescence microscopy.

For *ex vivo* transmigration in micro-Transwell system (Boyden chamber, Costar, 3 μm-diameter pore size membrane coated with fetal calf serum, in triplicate), lymphocyte preparations (4.10^5 cells/well) were added in the upper chambers and chemokines in the lower compartments: CXCL12 (10ng/ml), CCL5 (100ng/ml), CCL2 and CXCL10 (20ng/ml). Transwell were incubated at 37°C for 1.5-2h. In blockade experiments, anti-pep4 antibody CRMP2 blocking antibody (3 mg/mL) was added to the lymphocyte preparation for 30 min at 37°C just before transmigration assay as already reported (Vincent et al., 2005). Migratory cells in the lower chambers or in hippocampus slices were counted under the microscope. Data were expressed as total number of migratory T cells.

Statistical analysis

Statistical significance in comparing two means was tested with the unpaired Student's *t* test, *p* values<0.05 were considered significant. In the migration test, the number of migratory lymphocytes was counted by light microscopy (15-20 microscope fields per condition -2 or 3 independent experiments) and data expressed as mean number of migratory lymphocytes per field.

3- **Results**

Neuronotropic RABV and CDV infections trigger the stimulation of CRMP2+ cell populations in the periphery

Mouse models of virus-induced encephalitis, RABV and CDV were developed using two different strains of mice, C57B6 and SV129. Preliminary analysis indicated that the basal expression of CRMP2 in immune cells in healthy C57B6 and SV129 mice was different. While in healthy BALBC mice, less than 20 % of PBMC and lymph node mononuclear cells expressed CRMP2, virtually all PBMC and lymph node mononuclear cells of SV129 mice expressed CRMP2 (98.6±0.7% positive cells). To investigate how RABV and CDV infections regulate CRMP2 in these two strains of mice, CRMP2 expression was investigated by cytofluorimetry in PBMC and lymph nodes mononuclear cells of BALB/C and SV129 mice during the course of RABV or CVD infection, respectively.

BALB/C mice were infected with three different types of laboratory RABV strains: CVS, PV and ERA. These strains are different in respect of neurotropism and issue of the disease. ERA is a vaccine virus strain, which has lost the property to infect the nervous system after peripheral infection in BALB/c mice. PV is a neuronotropic virus causing only abortive rabies (Galelli et al., 2000) as mice are paralyzed but survived. In contrast, CVS is a neuronotropic virus strain causing a fatal myelo-encephalitis (Baloul et al., 2004). PBMC and lymph nodes were sampled at different times (days 1, 7 and 9) after intramuscular injection with RABV or injection of medium only (non-infected mice). After CVS inoculation, infection did not significantly modify the % of $CD3^+$ cells among the PBMC of BALB/c mice during the time period (days 1, 7 and 9) of the infection (Figure 1-A). In contrast, the percentage of cells expressing CD69, this molecule being taken as a marker of early activation (Hamann et al., 1993), increased significantly on day 7 before declining thereafter, suggesting that infection with CVS triggered the transient activation of PBMC (Figure 1-A). In parallel, a drastic increase in $CRMP2^+$ cells among the PBMC of CVS-infected animals occurred at day 7 (78% of the PBMC in infected animals expressed CRMP2 compared to less than 20% in non-infected animals) (Figure 1A). This increase was still high (70%) on the 9^{th} day of infection. The CRMP2+ cells recruited among the CD3+ T lymphocytes and activated CD69+ cell subsets, as shown by double-staining analysis (80% of CRMP2+ cells from CVS infected animals at day 7 were CD3+ and 20% were CD69+) (Figure 1-B). Virtually all CD69+ cells (98.7±1.2%) triggered by the infection at day 7 and most CD3+ T cells (75.4±2.8%) expressed CRMP2. In addition, the frequency of T lymphocytes expressing CRMP2

increased with time (20% on day 1, 70-80% on days 7 and 9, respectively (Figure 1-C). Similar patterns were obtained with popliteal lymph nodes (data not shown). After infection with PV, a neuronotropic RABV strain causing abortive rabies, similar expansion of CRMP2+ cells was observed in PBMC than those observed after CVS infection (Figure 1D). In contrast, after infection with the non-neuronotropic RABV strain ERA, the number of cells expressing CRMP2 remained unchanged in the course of the infection and not different from those observed in non-infected mice. However, expansion of CD69 positive cells was similar in ERA to those observed in PV infected mice, suggesting that the early steps of T cell activation have occurred after ERA infection as they have occurred after PV and CVS infection. This suggests that CRMP2 expression by lymphocytes in periphery is associated with RABV neurotropism.

Altogether, these data indicated that neurotropic strains of RABV triggered CRMP2 expression in peripheral T lymphocytes and that most of the early-activated cells (CD69+), which increase in number through infection, also expressed CRMP2.

CRMP2 expression was then evaluated in a model of mice infected by intracerebral injection of a mice-adapted neurovirulent CDV strain previously shown to infect neurons (Bernard et al., 1993). In CDV infected SV129 mice, PBMC and lymph nodes were sampled at different times (day 3, 7, 11 and 14) following injection of neuro-adapted virus (infected-mice) or brain suspension (sham-inoculated mice). At first, a significant decline was detected in the CD3+ lymphocyte frequency in PBMC on day 7 post virus-inoculation (47.2% versus 63.3% in sham mice), probably due to the immunosuppressive effect of CDV (Figure 2-A). Nevertheless and similarly to what was observed in RABV infected mice, the frequency of CD69+ cells among PBMC increased (10.5% versus 5.2% in sham mice on day 7 post-inoculation). When CRMP2 expression was analyzed in terms of CRMP2+ cell frequency (% of positive cells in the total population), CDV infection did not modify the % of CRMP2 expressing cells (≈98% positive cells, not shown). In contrast, when the CRMP2 level per cell (mean fluorescence intensity= MIF) was analyzed in double stained cells (Figure 2-B), CRMP2 expression showed an increase in MIF in CD3+ and CD69+ cells of CDV-infected mice, reaching significance on day 7 post-inoculation. Focusing on the CD69+CRMP2+ subpopulation (Figure 2-C), cytofluorimetry analysis indicated that CDV infection triggered the expansion of a discrete population characterized by a strong CRMP2 and CD69 expression. This cell subset, termed CRMP2hi, was recruited preferentially among the activated cell population CD69+, was characterized by an elevated CRMP2 expression (MIF for

CRMP2hi cell population= 26-45 vs 16-20 for non-CRMP2hi cells) and constituted 57±13% of the CD69+CRMP2+ cell population and so, probably participated to the elevated mean fluorescence intensity detected in CD69+ activated cells of infected mice. CRMP2hi cells were specifically detected in PBMC and lymph node of the infected animals, at the peak of encephalitis, namely on day 7 (in 9 out 12 infected mice analyzed) and on day 11 post-inoculation (in 4 out 5 infected mice analyzed) (Figure 2-D). Thus, even under conditions of CRMP2 constitutive expression, CDV infection increased CRMP2 level in a subset of activated cells in blood and lymph nodes.

In conclusion, analysis of CRMP2 expression in peripheral immune cells performed in different models of viral infection indicated that neurotropic strains of CDV and RABV specifically increased the level of CRMP2 in circulating lymphocytes. Depending on the constitutive level of CRMP2 expression, neural infection triggered the expansion of CRMP2+ or CRMP2hi cell populations. These CRMP2+ cells recruited mainly among CD3+ T lymphocytes, notably in CD69+ early-activated cells.

Selective recruitment of CRMP2+CD3 T cells in neurovirulent RABV and CDV infected CNS

Assuming that elevated CRMP2 expression may favor T cell motility and transmigration to inflamed tissue, we analyzed whether CRMP2+ cells expansion in the periphery after RABV or CDV inoculation correlated with trafficking to the CNS as the viral infection progressed in this tissue. Mononuclear cells were isolated from the CNS using Percoll gradients and phenotyped by cytofluorimetry, at different times after viral inoculation. In the RABV infection model with the neurovirulent strain CVS we focused our analysis on CD3+ T cells, which selectively migrate into the CNS of infected mice (Figure 3-A). In the absence of infection and also in the first 5 days of CVS infection, CD3+ T cells could only be detected in minimal amounts (10-15% of the Percoll-collected cells), whereas later in the infection, CD3+ T cells constituted 30% (day 8) and up to 60% (day 12) of the migratory cells. Double staining analysis (CRMP2 and CD3) showed a recruitment of CRMP2+CD3+ T cells in the CNS on day 8 (27% of the Percoll-collected cells). This percentage was unchanged on day 12 (Figure 3-B). The combination of the CRMP2+ Percoll collected cell population was further investigated by double staining of CRMP2 with markers chosen to roughly identify B-lymphocytes (B220), T-lymphocytes (CD3), monocyte/macrophages and microglia (CD11b), NK and dentritic cells (CD11c), on days 0, 5, 8 and 12 post-infection. At each time point, the total % of CRMP2+ cells was taken as 100 and the frequencies of B220, CD11C, CD11b and CD3 were calculated (Figure 3-C). Under non-infected

conditions, CRMP2+ cells could be sorted into CD11b (80%) and B220 (20%) in the brain. CVS infection modified these ratio, inducing a drastic increase in CD3+CRMP2+ cells (38% and 62% are T lymphocytes on days 8 and 12, respectively), a decrease of B220+CRMP2+ cells and the appearance of a CD11c+CRMP2+ cell population accounting for a small percentage of the CRMP2+ population (peak 12% on day 8). CD11b antigen, a marker of both macrophages and microglia, could not differentiate the resident microglia trapped in the Percoll preparation from infiltrated immune phagocytes.

Cytofluorimetry analysis of Percoll-collected cells was further performed in the mouse model of CDV infection on days 7 and 14 post-infection. Compared to non-infected conditions, the frequency of CD3+ T-lymphocytes and early-activated CD69+ cells detected in the brain infiltrate was significantly enhanced under CDV infection (reaching significance on day 14) (Figure 4-A), indicating that in the course of CNS infection, inflamed brain attracts immune cells. Co-detection of CRMP2 with CD69 and CD3 antigens on migratory cells showed that almost all expressed high CRMP2 levels, thus behaving like CRMP2high cells (illustration of one infected-brain and sham-inoculated brains in Figure 4-B). Immunocytochemistry performed on brain slices from mice examined on day 14 post-inoculation confirmed that CRMP2+ cells mainly infiltrated the infected neural tissue (Figure 5-A) and showed the accumulation of CD4+ T lymphocytes in the parenchyma of several brain structures previously demonstrated to replicate CDV, including hippocampus and thalamus (Bernard et al., 1993) (Figure 5-B). T lymphocytes, in particular, were present in brain parenchyma, at the proximity of structures involved in blood-CNS exchange: the *velum interpositum* of meninges, the choroid plexuses in ventricle. Immunofluorescence assay detected CD4+ and CD8+ cells in ethanol fixed neural tissue, confirming the presence of T lymphocytes in the brain infiltrate of CDV infected mice (Figure 5-C). Co-detection of CRMP2 and CD4 or CD8 antigens on brain slices could not be performed (different tissue fixation requirement). However, CRMP2 and TCR beta chain positive cells were co-detected in same brain areas (acetone fixation) (Figure 5C) confirming the presence of CRMP2+ lymphocytes in infected/inflamed brain.

Altogether, these observations supported the idea that infection of the CNS with a neurotropic virus modifies CRMP2 expression in activated immune cells in the periphery, and favored the recruitment, mainly of CRMP2+ T-lymphocytes, to the infected brain.

Enhanced migratory rates for peripheral immune cells displaying elevated CRMP2 expression in CDV-infected mice

As brain infiltration may result from the elevated migratory rate and/or enhanced survival of activated immune cells within neural tissue, the effect of CNS viral infection on the motility of peripheral immune cells was investigated *ex vivo* on T-lymphocytes isolated from lymph nodes on day 7 post inoculation (3 infected- and 3 non-infected mice tested). Immune cells from lymph nodes were first analyzed for CRMP2 expression. Cytofluorimetry detected a clear increase in CRMP2 expression level (Figure 6-A) and the presence of CRMP2hi cells (38.3 to 77.2% of the total CD69+CRMP2+ cells) in CDV-infected mice. The migratory rate was further analyzed, as previously reported (Vincent et al., 2005), in a Transwell chamber system allowing the determination of the number of cells migrating towards a gradient of chemokines known to be present in virus-infected inflamed brain (CXCL12, CCL5, CXCL10) (Patterson et al., 2003). As shown in Figure 6-B, lymphocytes from CDV-infected mice displayed a greater migratory rate compared to those isolated from non-infected mice (89,1±4 versus 43,7±17 migrating cells). In blockade experiment using an anti-CRMP2 antibody previously shown to lower T cell migration, the migratory rate was reduced by 30% and 10% for lymphocytes of CDV- and sham-inoculated mice, respectively. The ability for lymphocyte to migrate to CNS tissue was further examined *ex vivo* using mouse hippocampus maintained in organotypic culture (Figure 6-C). Brain slices were either non-infected or infected with CDV for three days before migration assay. Lymphocytes from lymph nodes of CDV-infected and sham-inoculated mice were stained with vital dye CFSE (1μM) then spotted close to CDV- and non-infected brain slices. Following 18h incubation, migrating lymphocytes were detected on brain slices (Figure 6-C). Compared to lymphocytes of sham-inoculated mice, lymphocytes of CDV-infected mice greatly invaded the CDV-infected brain slices (Figure 6-C and graph in 6-D). Following treatment with anti-CRMP2 antibody, lymphocytes of CDV- and sham-inoculated mice displayed similar migratory rates, demonstrating the role of CRMP2 in the elevated ability to traffic to neural tissue displayed by CDV-infected mice lymphocytes.

All these experiments indicated that virus-induced elevated CRMP2 expression conferred to lymphocytes a greater ability to migrate into neural tissue, thus increasing the potential of T cells to target infected/inflamed brain.

Presence of peripheral CRMP2hi cells correlates with the severity of clinical scores in mice suffering from RABV encephalitis

In contrast to mice infected with CDV, which develop abrupt signs of encephalitis, RABV-infected mice displayed progressive and well-scored clinical signs (Camelo et al., 2001b), allowing a correlative study between clinical score and CRMP2 expression levels in the periphery. After intra-muscular injection with the highly neurotropic strain of RABV, CVS-1, BALB/c mice develop fatal acute encephalitis. The first symptoms (ruffled fur, muscle stiffness) detected at day 6 post-infection (pi) were quickly followed by paralysis of the hind limbs and then forelimbs, hunch back, severe loss of weight and prostration followed by death (day 13 pi). A representative evolution of the cumulative scores (addition of individual scores of the 8 animals of the group) after RABV injection is presented in Figure 7-A. To analyze the time course of CRMP2 expression in the peripheral immune cells, together with the clinical score, RABV infected mice were bled and sacrificed at different times post infection and individual clinical scores at the time of sacrifice were recorded. CRMP2 expression levels in PBMC and lymph node cells were then evaluated by cytofluorimetry. Similar to the CDV infection model, CRMP2hi cells were detected in infected mice, as shown by the high CRMP2 expression in the CD3+ T lymphocyte population of infected compared to non-infected mice (Figure 7-B). When CRMP2hi cells were plotted against the individual clinical score displayed by encephalitic mice (Figure 7-C), they appeared preferentially in sick mice displaying high clinical scores (>3-5). Indeed, a significant correlation between the cumulative clinical scores displayed by RABV-infected mice and the frequency of CRMP2+ cells in blood (R^2= 0.69) was detected using a logarithmic representation of non-linear regression analysis (Figure 7-D). After infection with the neuronotropic RABV strain, PV, causing abortive RABV and sustained infiltration of T cells into the CNS (Galelli et al., 2000), the correlation index was 0,78. This strongly suggested the participation of CRMP2hi cells in the deleterious neuroinflammatory reaction induced in the infected CNS, and indicated CRMP2 expression levels in PBMC as a potential peripheral marker of virus-induced neuroinflammation.

Collectively, our data revealed an association between clinical features and the presence, both in the periphery and in the brain of mice suffering from virus-induced encephalitis, of activated T-lymphocytes displaying high CRMP2 levels.

4- Discussion

In the present study, we showed that brain infection by neurovirulent strains of two viruses, either RABV or CDV, causing fatal encephalitis, triggers CRMP2 expression in activated T lymphocytes.

These cells of increased mobility find their way to the infected brain. CRMP2 expression by T cells seems to be a hallmark of infection/inflammation of the brain, since it was not observed after infection with non-neurovirulent RABV infection. Interestingly, the kinetics of CRMP2 expression in the periphery reflected the severity of the brain disease.

Following intramuscular (IM) inoculation, neurovirulent strains of RABV induced local (popliteal lymph node) and systemic (spleen) proliferative and cytotoxic responses, with notably cytokine secreting T cells and specific RABV antibodies (Irwin et al., 1999). We showed here that, as early as 5 days post infection, the T cells of lymph nodes and blood were activated (CD69 expression) and expressed CRMP2. After intracerebral (IC) injection of CDV, a similar immune response was obtained, suggesting that viral inoculation by the IM and IC routes both activated the systemic immune response. This can be surprising as the nervous system is an immuno specialized organ where directly injected viruses evade an immune response, probably through the installation of an immunosuppressive milieu (Galea et al., 2007). However, this is not the case when antigens or virus particles are delivered by intrathecal immunization (Cserr et al., 1992; Cserr and Knopf, 1992; Harling-Berg et al., 1991; Panda et al., 1965; Stevenson et al., 1997; Shin et al., 2006). It is likely that after IC inoculation of the CDV, virus induced leakage of neural cells and redirected viral antigens to the cerebrospinal fluid, the meninges and finally to the cervical lymph nodes (Hatterer et al., 2006). Thus, despite the tropism of neurovirulent RABV and CDV to the CNS, initial viral entry into the body by the IM and IC routes triggered a strong immune response in the periphery and the induction of CRMP2 positive cells in secondary lymphoid organs that circulate further into the blood. After IM infection with a non-neurovirulent RABV strain, CRMP2 expansion was no observed. This does not result from an absence of immune activation since expansion of CD69+ cells was similar to those observed after neurovirulent RABV injection, nor from the route of injection since both groups of mice were injected IM. It may result of the capacity of the non neurovirulent RABV strain ERA to infect bone marrow macrophages (Ray et al., 1995) a property which is not shared by neurovirulent RABV strains which are strictly neuronotropic. This point would require further investigation.

How could CRMP2 integrate the multiple pathways involved in the homing and accumulation of T lymphocytes in the infected CNS? Access to the brain is strictly controlled by blood-brain interfaces, blood vessels and the choroid plexus, and accumulation in neural tissue may result from the enhanced entry/reduced exit rates of T cells from the brain (Kleine and Benes, 2006; Bechmann et al., 2007;

Engelhardt and Ransohoff, 2005). The activation process has a dramatic effect on this pathway, in particular by modulating the expression of the adhesion molecules, metalloproteases and chemokine receptors required for lymphocyte transendothelial migration and crawling in inflamed tissue (Barreiro et al., 2002; del Pozo et al., 1995; Giraudon et al., 1997; Lane et al., 2000; Strazielle et al., 2003). As a result, more resting T-cells are found in lymphoid organs while activated T-cells mainly target non-lymphoid organs, including brain (Westermann et al., 2005). In RABV- and CDV-infected mice, the presence of early-activated cells and T lymphocytes displaying high CRMP2 levels, associated with high migratory rates for T lymphocytes, suggests that the activation process may modulate T cell motility through CRMP2 modulation. Our recent observations support this hypothesis. An association between CRMP2 expression levels, T-cell activation status and *in vitro* cell migratory rates was observed in patients suffering from virus-induced neuroinflammatory disease (Vincent et al., 2005). In addition, T-cell activation through CD3-CD28 stimulation clearly enhanced CRMP2 levels per cell (unpublished data). How CRMP2 operates in activated T-lymphocytes to drive their migration to the CNS is currently under investigation. The role of CRMP2 in the CNS provides some clues to understanding its function in the immune system. By its ability to associate with cytoskeletal elements, CRMP2 participates in the cytoskeletal reorganization required for neuronal cell reshaping and migration under semaphorin signals through the promotion of microtubule extensions (Fukata et al., 2002), a process inactivated by CRMP2 phosphorylation (Yoshimura et al., 2005; Cole et al., 2006; Uchida et al., 2005). In immune cells, we have shown the ability of CRMP2 to bind vimentin and tubulin (Vincent et al., 2005) thus to participate in lymphocyte reshaping. Inflammatory molecules, notably chemokines, could act as modulators of CRMP2 function, promoting T cell reshaping and motility in neuroinflammatory situations. This idea is supported by the role and distribution of ckemokines in the inflamed/infected brain. Indeed, chemokines are required for lymphocyte chemotaxis through actomyosin/ microtubule organization (Vicente-Manzanares and Sanchez-Madrid, 2004; Rey et al., 2002). Chemokines regulate cell entry into the brain microvasculature, direct navigation across the Virchow-Robin perivascular space and facilitate T cell crawling in brain parenchyma (Kleine and Benes, 2006; Lane et al., 2000; Lee et al., 2004; Liu et al., 2000; Ransohoff et al., 2003). Chemokines are expressed at high levels in the virus infected CNS, as it is the case after RABV infection (Baloul and Lafon, 2003; Roy et al., 2007; Wang et al., 2005).

In several infection models, the infiltration of activated T-lymphocytes into the brain is a well-characterized parameter linked to the development of encephalitis and neurodegeneration (Irani and Griffin, 1991; Khuth et al., 2001; Marten et al., 2003). A priming process initiated by a low number of infiltrating encephalitogenic T-lymphocytes could set the stage for a second greater wave of invading effector cells, as observed in multiple sclerosis patients and associated animal models (Engelhardt and Ransohoff, 2005; Norman and Hickey, 2005). The subsequent induction of a shift towards a pro-inflammatory CNS microenvironment may have beneficial/unfavorable consequences, leading to viral clearance but promoting immune-related damage to neural cells (Fujinami et al., 2006; Griffond et al., 2004). Whether or not T cells contribute to immunopathology in RABV is still controversial and seems to depend upon strain pathogenicity (Camelo et al., 2001b; Galelli et al., 2000; Hooper, 2005; Lafon, 2005). In CDV-infected mice, clinical and histological changes in the CNS do not develop immediately upon viral inoculation but only after a latency period, coinciding with T lymphocyte infiltration (Khuth et al., 2001). This suggests that infiltrating immune cells are important effectors of the intrathecal deleterious process translated in clinical manifestations.

The association we observed between CRMP2 expression in peripheral immune cells, in particular the presence of CRMP2hi cells, and the clinical scores displayed by encephalitic infected mice and the fact this is restricted to the infection of brain (not seen after the non neurovirulent RABV infection) suggest that CRMP2 could be used as a cell marker to isolate and profile the cells with the potential to infiltrate the infected CNS. This could help in decrypting the association of migrating lymphocytes with the complex process leading to lethal encephalitis or recovery. Bearing early-activated T-lymphocyte and dendritic cell markers, CRMP2hi cells could comprise active cytolytic CD8+ T-lymphocytes, regulatory CD4+ T cells and antigen-presenting cells, each displaying their own role. They could therefore be crucial either in controlling the immune response to pathogens and virus clearance or in preventing reactivity to self-antigens, thus reducing the autoimmune reaction within the CNS (Serafini et al., 2004; Serafini et al., 2006; Esiri, 2007; Lauterbach et al., 2006; Ramakrishna et al., 2006). Detailed analysis of selected CRMP2hi cells along the course of viral infection and disease would bring information on the nature and function of cells sequentially recruited to the inflamed CNS.

To conclude, the present work supports the idea that viral infection of the CNS enhances the ability of activated T-lymphocytes to switch on the intracellular machinery that recruits the cytoskeletal reorganizer CRMP2 and triggers cell migration. This also identifies CRMP2 molecule as a potential

marker of activated and motile T-lymphocytes generated during viral infection and potentially recruited in the inflamed CNS.

References

Baloul, L., Camelo, S., Lafon, M., 2004. Up-regulation of Fas ligand (FasL) in the central nervous system: a mechanism of immune evasion by rabies virus. J Neurovirol 10, 372-382.

Baloul, L., Lafon, M., 2003. Apoptosis and rabies virus neuroinvasion. Biochimie 85, 777-788.

Barreiro, O., Vicente-Manzanares, M., Urzainqui, A., Yanez-Mo, M., Sanchez-Madrid, F., 2004. Interactive protrusive structures during leukocyte adhesion and transendothelial migration. Front Biosci 9, 1849-1863.

Barreiro, O., Yanez-Mo, M., Serrador, J.M., Montoya, M.C., Vicente-Manzanares, M., Tejedor, R., Furthmayr, H., Sanchez-Madrid, F., 2002. Dynamic interaction of VCAM-1 and ICAM-1 with moesin and ezrin in a novel endothelial docking structure for adherent leukocytes. J Cell Biol 157, 1233-1245.

Bechmann, I., Galea, I., Perry, V.H., 2007. What is the blood-brain barrier (not)? Trends Immunol 28, 5-11.

Bencsik, A., Malcus, C., Akaoka, H., Giraudon, P., Belin, M.F., Bernard, A., 1996. Selective induction of cytokines in mouse brain infected with canine distemper virus: structural, cellular and temporal expression. J Neuroimmunol 65, 1-9.

Bernard, A., Cohen, R., Khuth, S.T., Vedrine, B., Verlaeten, O., Akaoka, H., Giraudon, P., Belin, M.F., 1999. Alteration of the leptin network in late morbid obesity induced in mice by brain infection with canine distemper virus. J Virol 73, 7317-7327.

Bernard, A., Fevre-Montange, M., Bencsik, A., Giraudon, P., Wild, T.F., Confavreux, C., Belin, M.F., 1993. Brain structures selectively targeted by canine distemper virus in a mouse model infection. J Neuropathol Exp Neurol 52, 471-480.

Bretin, S., Reibel, S., Charrier, E., Maus-Moatti, M., Auvergnon, N., Thevenoux, A., Glowinski, J., Rogemond, V., Premont, J., Honnorat, J., Gauchy, C., 2005. Differential expression of CRMP1, CRMP2A, CRMP2B, and CRMP5 in axons or dendrites of distinct neurons in the mouse brain. J Comp Neurol 486, 1-17.

Brown, M.J., Hallam, J.A., Colucci-Guyon, E., Shaw, S., 2001. Rigidity of circulating lymphocytes is primarily conferred by vimentin intermediate filaments. J Immunol 166, 6640-6646.

Camelo, S., Castellanos, J., Lafage, M., Lafon, M., 2001a. Rabies virus ocular disease: T-cell-dependent protection is under the control of signaling by the p55 tumor necrosis factor alpha receptor, p55TNFR. J Virol 75, 3427-3434.

Camelo, S., Lafage, M., Galelli, A., Lafon, M., 2001b. Selective role for the p55 Kd TNF-alpha receptor in immune unresponsiveness induced by an acute viral encephalitis. J Neuroimmunol 113, 95-108.

Carlson, N.G., Hill, K.E., Tsunoda, I., Fujinami, R.S., Rose, J.W., 2006. The pathologic role for COX-2 in apoptotic oligodendrocytes in virus induced demyelinating disease: implications for multiple sclerosis. J Neuroimmunol 174, 21-31.

Charrier, E., Reibel, S., Rogemond, V., Aguera, M., Thomasset, N., Honnorat, J., 2003. Collapsin response mediator proteins (CRMPs): involvement in nervous system development and adult neurodegenerative disorders. Mol Neurobiol 28, 51-64.

Cole, A.R., Causeret, F., Yadirgi, G., Hastie, C.J., McLauchlan, H., McManus, E.J., Hernandez, F., Eickholt, B.J., Nikolic, M., Sutherland, C., 2006. Distinct priming kinases contribute to differential regulation of collapsin response mediator proteins by glycogen synthase kinase-3 in vivo. J Biol Chem 281, 16591-16598.

Cserr, H.F., Harling-Berg, C.J., Knopf, P.M., 1992. Drainage of brain extracellular fluid into blood and deep cervical lymph and its immunological significance. Brain Pathol 2, 269-276.

Cserr, H.F., Knopf, P.M., 1992. Cervical lymphatics, the blood-brain barrier and the immunoreactivity of the brain: a new view. Immunol Today 13, 507-512.

del Pozo, M.A., Sanchez-Mateos, P., Nieto, M., Sanchez-Madrid, F., 1995. Chemokines regulate cellular polarization and adhesion receptor redistribution during lymphocyte interaction with endothelium and extracellular matrix. Involvement of cAMP signaling pathway. J Cell Biol 131, 495-508.

del Pozo, M.A., Vicente-Manzanares, M., Tejedor, R., Serrador, J.M., Sanchez-Madrid, F., 1999. Rho GTPases control migration and polarization of adhesion molecules and cytoskeletal ERM components in T lymphocytes. Eur J Immunol 29, 3609-3620.

Engelhardt, B., Ransohoff, R.M., 2005. The ins and outs of T-lymphocyte trafficking to the CNS: anatomical sites and molecular mechanisms. Trends Immunol 26, 485-495.

Esiri, M.M., 2007. The interplay between inflammation and neurodegeneration in CNS disease. J Neuroimmunol 184, 4-16.

Fujinami, R.S., von Herrath, M.G., Christen, U., Whitton, J.L., 2006. Molecular mimicry, bystander activation, or viral persistence: infections and autoimmune disease. Clin Microbiol Rev 19, 80-94.

Fukata, Y., Itoh, T.J., Kimura, T., Menager, C., Nishimura, T., Shiromizu, T., Watanabe, H., Inagaki, N., Iwamatsu, A., Hotani, H., Kaibuchi, K., 2002. CRMP-2 binds to tubulin heterodimers to promote microtubule assembly. Nat Cell Biol 4, 583-591.

Galea, I., Bechmann, I., Perry, V.H., 2007. What is immune privilege (not)? Trends Immunol 28, 12-18.

Galelli, A., Baloul, L., Lafon, M., 2000. Abortive rabies virus central nervous infection is controlled by T lymphocyte local recruitment and induction of apoptosis. J Neurovirol 6, 359-372.

Giraudon, P., Buart, S., Bernard, A., Belin, M.F., 1997. Cytokines secreted by glial cells infected with HTLV-I modulate the expression of matrix metalloproteinases (MMPs) and their natural inhibitor (TIMPs): possible involvement in neurodegenerative processes. Mol Psychiatry 2, 107-110, 184.

Giraudon, P., Vincent, P., Vuaillat, C., Verlaeten, O., Cartier, L., Marie-Cardine, A., Mutin, M., Bensussan, A., Belin, M.F., Boumsell, L., 2004. Semaphorin CD100 from activated T lymphocytes induces process extension collapse in oligodendrocytes and death of immature neural cells. J Immunol 172, 1246-1255.

Griffond, B., Verlaeten, O., Belin, M.F., Risold, P.Y., Bernard, A., 2004. Specific alteration of the expression of selected hypothalamic neuropeptides during acute and late mouse brain infection using a morbillivirus: relevance to the late-onset obesity? Brain Res 1022, 173-181.

Hamann, J., Fiebig, H., Strauss, M., 1993. Expression cloning of the early activation antigen CD69, a type II integral membrane protein with a C-type lectin domain. J Immunol 150, 4920-4927.

Harling-Berg, C.J., Knopf, P.M., Cserr, H.F., 1991. Myelin basic protein infused into cerebrospinal fluid suppresses experimental autoimmune encephalomyelitis. J Neuroimmunol 35, 45-51.

Hatterer, E., Davoust, N., Didier-Bazes, M., Vuaillat, C., Malcus, C., Belin, M.F., Nataf, S., 2006. How to drain without lymphatics? Dendritic cells migrate from the cerebrospinal fluid to the B-cell follicles of cervical lymph nodes. Blood 107, 806-812.

Hooper, D.C., 2005. The role of immune responses in the pathogenesis of rabies. J Neurovirol 11, 88-92.

Irani, D.N., Griffin, D.E., 1991. Isolation of brain parenchymal lymphocytes for flow cytometric analysis. Application to acute viral encephalitis. J Immunol Methods 139, 223-231.

Irwin, D.J., Wunner, W.H., Ertl, H.C., Jackson, A.C., 1999. Basis of rabies virus neurovirulence in mice: expression of major histocompatibility complex class I and class II mRNAs. J Neurovirol 5, 485-494.

Khuth, S.T., Akaoka, H., Pagenstecher, A., Verlaeten, O., Belin, M.F., Giraudon, P., Bernard, A., 2001. Morbillivirus infection of the mouse central nervous system induces region-specific upregulation of MMPs and TIMPs correlated to inflammatory cytokine expression. J Virol 75, 8268-8282.

Kleine, T.O., Benes, L., 2006. Immune surveillance of the human central nervous system (CNS): different migration pathways of immune cells through the blood-brain barrier and blood-cerebrospinal fluid barrier in healthy persons. Cytometry A 69, 147-151.

Lafon, M., 2004. Subversive neuroinvasive strategy of rabies virus. Arch Virol Suppl, 149-159.

Lafon, M., 2005. Modulation of the immune response in the nervous system by rabies virus. Curr Top Microbiol Immunol 289, 239-258.

Lane, T.E., Liu, M.T., Chen, B.P., Asensio, V.C., Samawi, R.M., Paoletti, A.D., Campbell, I.L., Kunkel, S.L., Fox, H.S., Buchmeier, M.J., 2000. A central role for CD4(+) T cells and RANTES in virus-induced central nervous system inflammation and demyelination. J Virol 74, 1415-1424.

Lauterbach, H., Zuniga, E.I., Truong, P., Oldstone, M.B., McGavern, D.B., 2006. Adoptive immunotherapy induces CNS dendritic cell recruitment and antigen presentation during clearance of a persistent viral infection. J Exp Med.

Lee, B.C., Lee, T.H., Avraham, S., Avraham, H.K., 2004. Involvement of the chemokine receptor CXCR4 and its ligand stromal cell-derived factor 1alpha in breast cancer cell migration through human brain microvascular endothelial cells. Mol Cancer Res 2, 327-338.

Liu, M.T., Chen, B.P., Oertel, P., Buchmeier, M.J., Armstrong, D., Hamilton, T.A., Lane, T.E., 2000. The T cell chemoattractant IFN-inducible protein 10 is essential in host defense against viral-induced neurologic disease. J Immunol 165, 2327-2330.

Marten, N.W., Stohlman, S.A., Zhou, J., Bergmann, C.C., 2003. Kinetics of virus-specific CD8+ -T-cell expansion and trafficking following central nervous system infection. J Virol 77, 2775-2778.

Mitchison, T.J., Cramer, L.P., 1996. Actin-based cell motility and cell locomotion. Cell 84, 371-379.

Norman, M.U., Hickey, M.J., 2005. Mechanisms of lymphocyte migration in autoimmune disease. Tissue Antigens 66, 163-172.

Panda, J.N., Dale, H.E., Loan, R.W., Davis, L.E., 1965. Immunologic Response to Subarachnoid and Intracerebral Injection of Antigens. J Immunol 94, 760-764.

Patterson, C.E., Daley, J.K., Echols, L.A., Lane, T.E., Rall, G.F., 2003. Measles virus infection induces chemokine synthesis by neurons. J Immunol 171, 3102-3109.

Peterson, L.K., Fujinami, R.S., 2007. Inflammation, demyelination, neurodegeneration and neuroprotection in the pathogenesis of multiple sclerosis. J Neuroimmunol 184, 37-44.

Ramakrishna, C., Atkinson, R.A., Stohlman, S.A., Bergmann, C.C., 2006. Vaccine-induced memory CD8+ T cells cannot prevent central nervous system virus reactivation. J Immunol 176, 3062-3069.

Ransohoff, R.M., Kivisakk, P., Kidd, G., 2003. Three or more routes for leukocyte migration into the central nervous system. Nat Rev Immunol 3, 569-581.

Rey, M., Vicente-Manzanares, M., Viedma, F., Yanez-Mo, M., Urzainqui, A., Barreiro, O., Vazquez, J., Sanchez-Madrid, F., 2002. Cutting edge: association of the motor protein nonmuscle myosin heavy chain-IIA with the C terminus of the chemokine receptor CXCR4 in T lymphocytes. J Immunol 169, 5410-5414.

Ricard, D., Rogemond, V., Charrier, E., Aguera, M., Bagnard, D., Belin, M.F., Thomasset, N., Honnorat, J., 2001. Isolation and expression pattern of human Unc-33-like phosphoprotein 6/collapsin response mediator protein 5 (Ulip6/CRMP5): coexistence with Ulip2/CRMP2 in Sema3a- sensitive oligodendrocytes. J Neurosci 21, 7203-7214.

Ray NB, Ewalt LC, Lodmell Rabies virus replication in primary murine bone marrow macrophages and in human and murine macrophage-like cell lines: implications for viral persistence. J Virol. 1995 Feb;69(2):764-72.

Roy, A., Phares, T.W., Koprowski, H., Hooper, D.C., 2007. Failure to open the blood-brain barrier and deliver immune effectors to central nervous system tissues leads to the lethal outcome of silver-haired bat rabies virus infection. J Virol 81, 1110-1118.

Salazar-Mather, T.P., Hokeness, K.L., 2006. Cytokine and chemokine networks: pathways to antiviral defense. Curr Top Microbiol Immunol 303, 29-46.

Sanchez-Madrid, F., del Pozo, M.A., 1999. Leukocyte polarization in cell migration and immune interactions. Embo J 18, 501-511.

Serafini, B., Rosicarelli, B., Magliozzi, R., Stigliano, E., Aloisi, F., 2004. Detection of ectopic B-cell follicles with germinal centers in the meninges of patients with secondary progressive multiple sclerosis. Brain Pathol 14, 164-174.

Serafini, B., Rosicarelli, B., Magliozzi, R., Stigliano, E., Capello, E., Mancardi, G.L., Aloisi, F., 2006. Dendritic cells in multiple sclerosis lesions: maturation stage, myelin uptake, and interaction with proliferating T cells. J Neuropathol Exp Neurol 65, 124-141.

Shin, J.H., Sakoda, Y., Kim, J.H., Tanaka, T., Kida, H., Kimura, T., Ochiai, K., Umemura, T., 2006. Efficacy of intracerebral immunization against pseudorabies virus in mice. Microbiol Immunol 50, 823-830.

Stevenson, P.G., Bangham, C.R., Hawke, S., 1997. Recruitment, activation and proliferation of CD8+ memory T cells in an immunoprivileged site. Eur J Immunol 27, 3259-3268.

Strazielle, N., Khuth, S.T., Murat, A., Chalon, A., Giraudon, P., Belin, M.F., Ghersi-Egea, J.F., 2003. Pro-inflammatory cytokines modulate matrix metalloproteinase secretion and organic anion transport at the blood-cerebrospinal fluid barrier. J Neuropathol Exp Neurol 62, 1254-1264.

Tishon, A., Lewicki, H., Andaya, A., McGavern, D., Martin, L., Oldstone, M.B., 2006. CD4 T cell control primary measles virus infection of the CNS: regulation is dependent on combined activity with either CD8 T cells or with B cells: CD4, CD8 or B cells alone are ineffective. Virology 347, 234-245.

Uchida, Y., Ohshima, T., Sasaki, Y., Suzuki, H., Yanai, S., Yamashita, N., Nakamura, F., Takei, K., Ihara, Y., Mikoshiba, K., Kolattukudy, P., Honnorat, J., Goshima, Y., 2005. Semaphorin3A signalling is mediated via sequential Cdk5 and GSK3beta phosphorylation of CRMP2: implication of common phosphorylating mechanism underlying axon guidance and Alzheimer's disease. Genes Cells 10, 165-179.

Verlaeten, O., Griffond, B., Khuth, S.T., Giraudon, P., Akaoka, H., Belin, M.F., Fellmann, D., Bernard, A., 2001. Down regulation of melanin concentrating hormone in virally induced obesity. Mol Cell Endocrinol 181, 207-219.

Veyrac, A., Giannetti, N., Charrier, E., Reymond-Marron, I., Aguera, M., Rogemond, V., Honnorat, J., Jourdan, F., 2005. Expression of collapsin response mediator proteins 1, 2 and 5 is differentially regulated in newly generated and mature neurons of the adult olfactory system. Eur J Neurosci 21, 2635-2648.

Vicente-Manzanares, M., Cabrero, J.R., Rey, M., Perez-Martinez, M., Ursa, A., Itoh, K., Sanchez-Madrid, F., 2002. A role for the Rho-p160 Rho coiled-coil kinase axis in the chemokine stromal cell-derived factor-1alpha-induced lymphocyte actomyosin and microtubular organization and chemotaxis. J Immunol 168, 400-410.

Vicente-Manzanares, M., Sanchez-Madrid, F., 2004. Role of the cytoskeleton during leukocyte responses. Nat Rev Immunol 4, 110-122.

Vincent, P., Collette, Y., Marignier, R., Vuaillat, C., Rogemond, V., Davoust, N., Malcus, C., Cavagna, S., Gessain, A., Machuca-Gayet, I., Belin, M.F., Quach, T., Giraudon, P., 2005. A role for the neuronal protein collapsin response mediator protein 2 in T lymphocyte polarization and migration. J Immunol 175, 7650-7660.

Wang, Z.W., Sarmento, L., Wang, Y., Li, X.Q., Dhingra, V., Tseggai, T., Jiang, B., Fu, Z.F., 2005. Attenuated rabies virus activates, while pathogenic rabies virus evades, the host innate immune responses in the central nervous system. J Virol 79, 12554-12565.

Westermann, J., Bode, U., Sahle, A., Speck, U., Karin, N., Bell, E.B., Kalies, K., Gebert, A., 2005. Naive, effector, and memory T lymphocytes efficiently scan dendritic cells in vivo: contact

frequency in T cell zones of secondary lymphoid organs does not depend on LFA-1 expression and facilitates survival of effector T cells. J Immunol 174, 2517-2524.

Yoshimura, T., Kawano, Y., Arimura, N., Kawabata, S., Kikuchi, A., Kaibuchi, K., 2005. GSK-3beta reg

Legends

Figure 1: CRMP2 expression in peripheral blood mononuclear cells of RABV infected mice. A- After infection in the periphery with the neurovirulent RABV strain CVS (**A,B,C**) or with the neurovirulent and partially attenuated RABV strain PV or non neurovirulent RABV strain ERA (**D**), PBMC were collected from infected (black or grey histogram) and sham-infected (white histograms) mice 1, 7 and 9 days post infection (pi). Kinetics of CD3, CD69 and CRMP2 frequency among total viable PBMC (**A and D**), % of CD3 or CD69 positive cells among CRMP2 positive cells (**B**) and % of CRMP2+ cells among CD3 and CD69 positive cells (**C**) was followed by cytofluorimetry analysis using appropriate pairs of antibodies. **A, B, C**- infection with a neuronotropic CVS RABV strain causing fatal rabies. CRMP2+ cells recruit in CD3+ T lymphocytes and early activated immune cell populations. RABV infection triggers CRMP2 expression in CD3 T lymphocytes; virtually all CD69+ cells express CRMP2. **D**- Infection with a neuronotropic RABV strain, PV, causing abortive rabies (dark gray histograms, or infection with a non neuronotropic RABV strain ERA causing no CNS disease (light gray histograms). In contrast to the neuronotropic PV strain, ERA strain does not trigger the expansion of CRMP2+ in PBMC of infected mice. These data are representative of at least three independent experiments (±SD).

Figure 2: **CRMP2 expression in peripheral blood mononuclear cells of CDV infected mice.** After infection of brain with CDV (gray histograms) or sham-infection (white histograms), PBMC were collected and analyzed by cytofluorimetry as decribed above. **A**- Transient reduction of CD3+ T cells and elevation of early-activated immune cells CD69+ frequency induced by brain infection; **B**- Elevated CRMP2 expression in CD3+ T cells and early-activated CD69+ cells, as shown by increased Mean Fluorescence Intensity (MFI); **C**- Detection in infected mice of early-activated CD69+ cells with elevated CRMP2 expression (MFI≥twice MFI observed in sham-infected mice) called CRMP2hi; **D**- Expansion of CRMP2hi cells increased progressively as infection and disease progressed. These analyses are representative of three independent experiments (±SD).

Figure 3: Immune cells infiltration in the CNS of neurovirulent RABV CVS strain infected mice analyzed by cytofluorimetry. Cells infiltrating the CNS of CVS infected (gray histograms) and sham-infected (white histograms) were isolated by Percoll gradients, stained with appropriate pairs of antibodies and analyzed by cytofluorimetry. Kinetics of CD3+ T cell frequency (**A**) and double stained CD3 and CRMP2 cells (**B**) were followed 1, 5, 8 and 12 days after infection in infected (black histograms) and non-infected (white histograms) mice. **C**- The distribution of CRMP2 expressing cells among CD3, CD11c, CD11b and B220 positive cells from the CNS was analyzed in the course of RABV infection (5, 8 and 12 days pi) and compared to the non-infected control (day 0). T lymphocytes constitute the majority of infiltrated immune cells on day 12 post inoculation, while CD11c+ cells (corresponding roughly to dendritic cells) peaked on day 8. Each point of the curve includes two to three mice. Data were representative of three different experiments (±SD).

Figure 4: Immune cell infiltration in the CNS of CDV infected mice analyzed by cytofluorimetry. Cells infiltrating the CNS were collected (7 and 14 dpi) and analyzed by cytofluorimetry as described above**. A**- Elevated recruitment of early activated CD69+ and CD3+ T cells under viral infection (black

histograms) compared to sham-infected (white histograms); **B**- Population of CD3+ cells and CRMP2hi (CD69+ CRMP2+) cells (dashed circle) is expanded in CDV infected brain (right panels) compared to sham-inoculated (left panels) (representative data of three different experiments).

Figure 5: Analysis of the brain infiltrates in CDV-infected mice. Immunodetection of brain infiltrating immune cells was performed by immunofluorescence (**A and C**, brain removed and immediately frozen) and by DAB staining (**B**, mice perfused with PFA) on coronal brain sections using anti-CD4, CD8, CRMP2 and TCR beta chain antibodies. **A**- CRMP2+ infiltrating cells are more abundant in the brain of CDV-infected than sham-inoculated mice (microscope field x400). **B**- CD4+ T lymphocytes infiltrated in CDV-infected brain structures hippocampus, thalamus (Khuth et al., 2001) and at proximity of the blood-CNS (velum interpositum) and CSF-CNS (third ventricle) interfaces (avidiin-biotin peroxidase system) (microscope field x100 and x400). **C**- Identification in CDV infected brain of CD4+ and CD8+ lymphocytes (microscope field x200) and CRMP2 expression by T lymphocytes (TCR beta chain positive cells) (microscope field x400).

Figure 6: Association of elevated CRMP2 expression with high migratory rate of lymphocytes collected in CDV infected mice: CRMP2 expression was evaluated by cytofluorimetry in lymph node cells of CDV-infected compared to non-infected mice prior to migration tests were performed in Transwell system (**B**) and on hippocampus organotypic culture **(C). A-** Elevated CRMP2 expression level (MFI) in lymphocytes of CVD-infected mice. **B-** Elevated migration of lymph node cells of CDV-infected mice (3 non-infected versus 3 CDV-infected mice) in a Transwell system (3μm pore membrane) in the presence of a chemokine gradient (CXCL12 -10ng/ml, CCL5 -100ng/ml, CCL2 and CXCL10 -20ng/ml, 37°C, 2h) (±SD). **C**- Migration analysis of lymph node cells stained with CFSE then spotted close to CDV-and non-infected hippocampus slices (18h contact then cell counting): elevated migratory rate of lymphocytes of CDV-infected versus sham-inoculated mice. Blockade experiment: treatment of lymphocytes with anti-CRMP2 antibody prior migration assay impeded tissue infiltration both on CDV-infected and non-infected hippocampus slices (open marks in graph).

Figure 7: Peripheral expansion of CRMP2hi cells in RABV infected mice correlates with clinical score: A- After infection, RABV infected animals develop clinical symptom which aggravate as the virus infectionprogresses into the NS. Progression was evaluated by scoring mobility and mortality as follows: 0=normal mice, 1=ruffled fur, 2=loss of agility, 3=one paralyzed hind leg, 4=two paralyzed hind legs, 5=total loss of mobility and 6=death. A representative evolution of the cumulative clinical scores (addition of individual scores of 8 animals per group); **B**- CD3+ T cells expressing strong CRMP2 fluorescence (CRMP2 high) can be observed in lymph node cells of infected animals (right panel showing CD3/CRMP2 expression in lymph nodes of 7 day RABV infected mice). These cells were absent in the CD3+ T cells of non-infected mice (middle panel) (representative data). **C**- CRMP2hi cells can be detected not only in lymph nodes but also in PBMC as the disease (individual clinical score on x axis) progresses (4 mice represented); **D**- When individual clinical scores were plotted against % of CRMP2+CD3+ T cells in lymph node, a significant correlation was observed (R= 0.69) between CRMP2 cells and individual clinical scores (logarithmic representation of non-linear regression analysis).

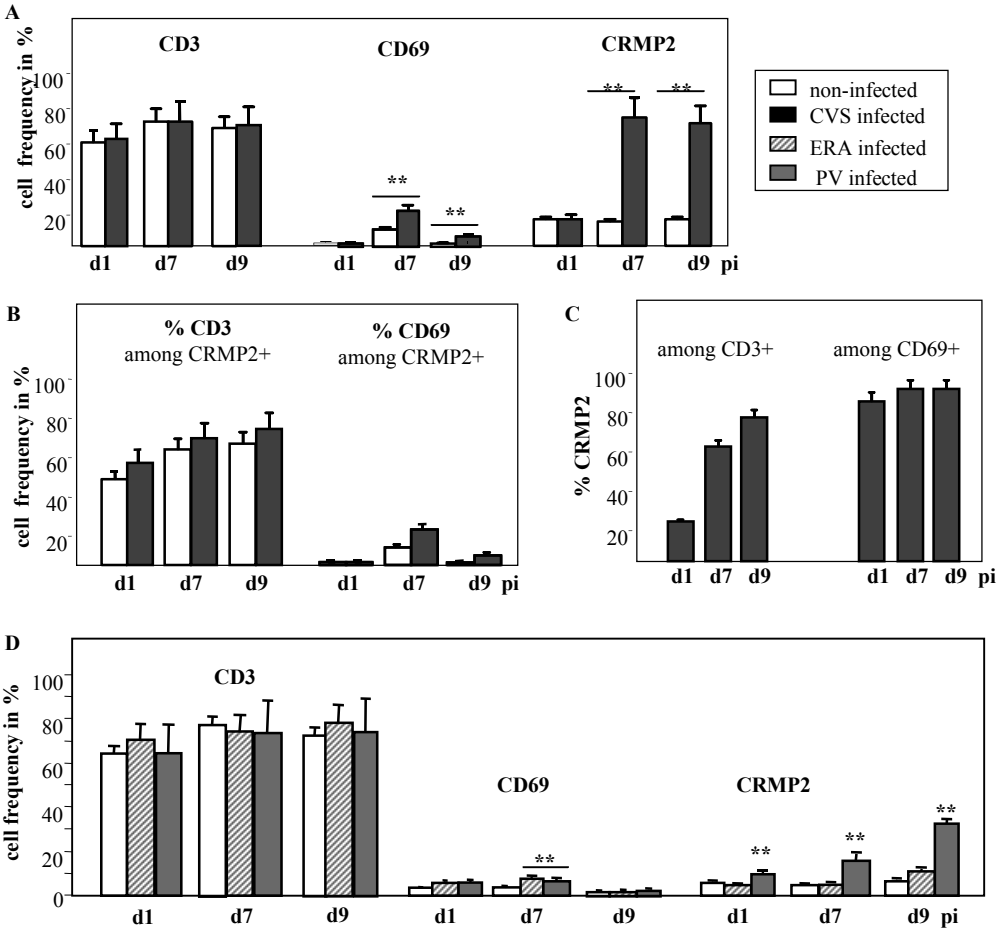

Figure-1, Vuaillat et al

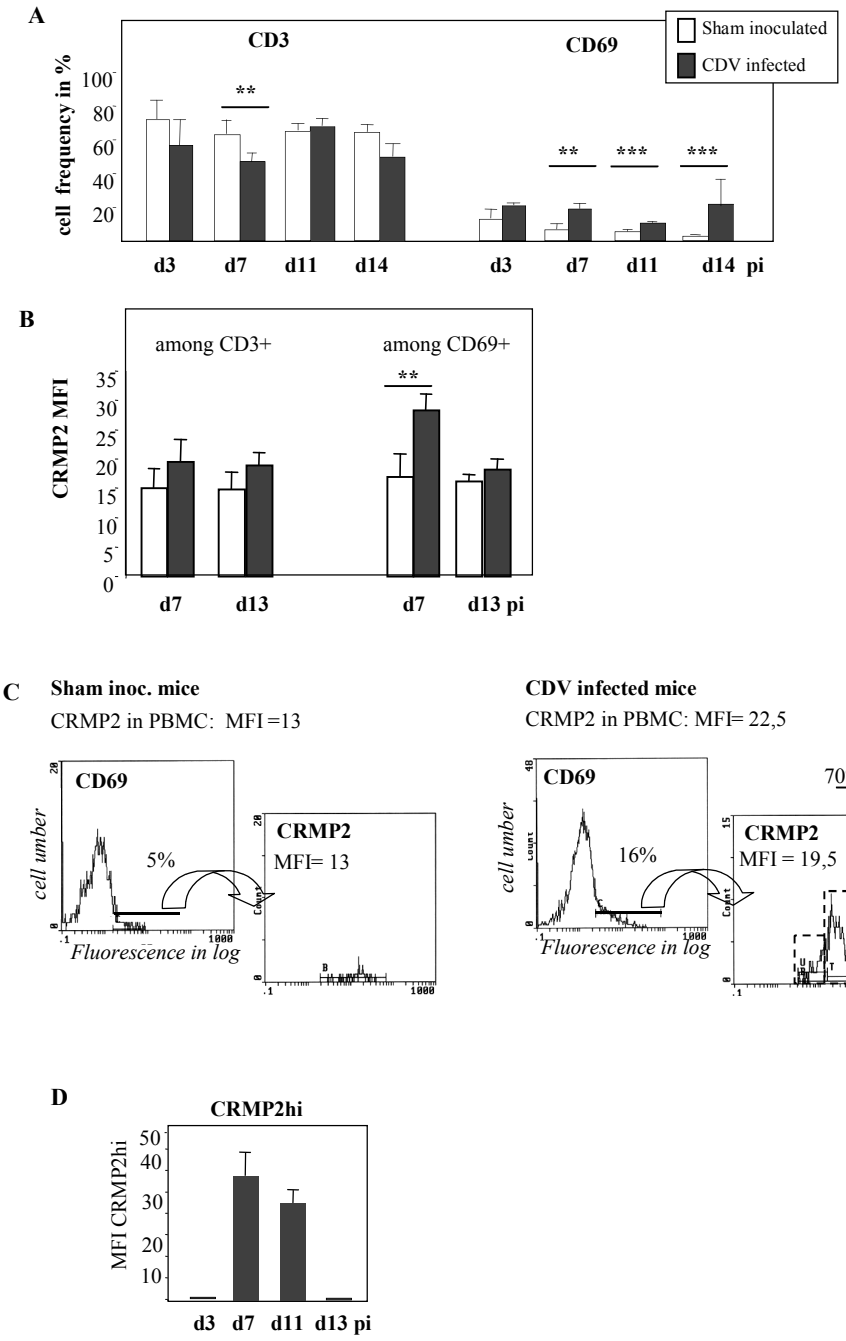

Figure-2 , Vuaillat et al

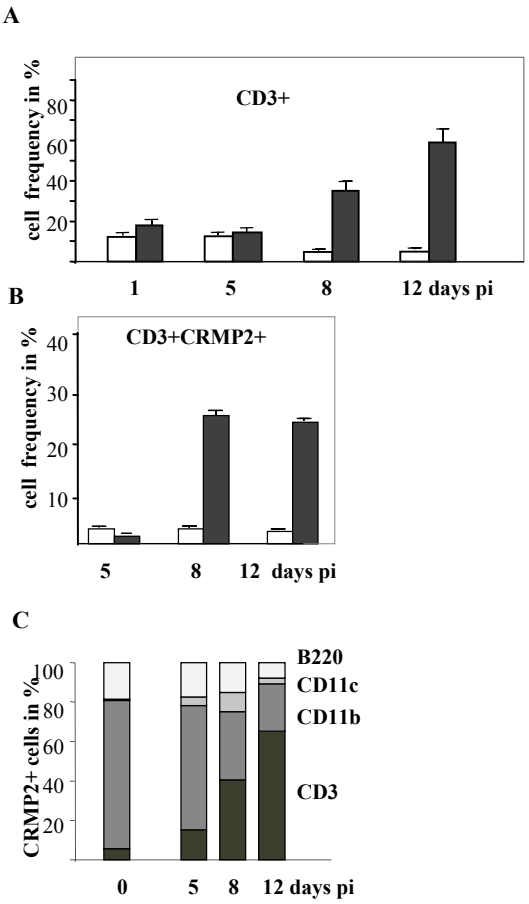

Figure-3 , Vuaillat et al

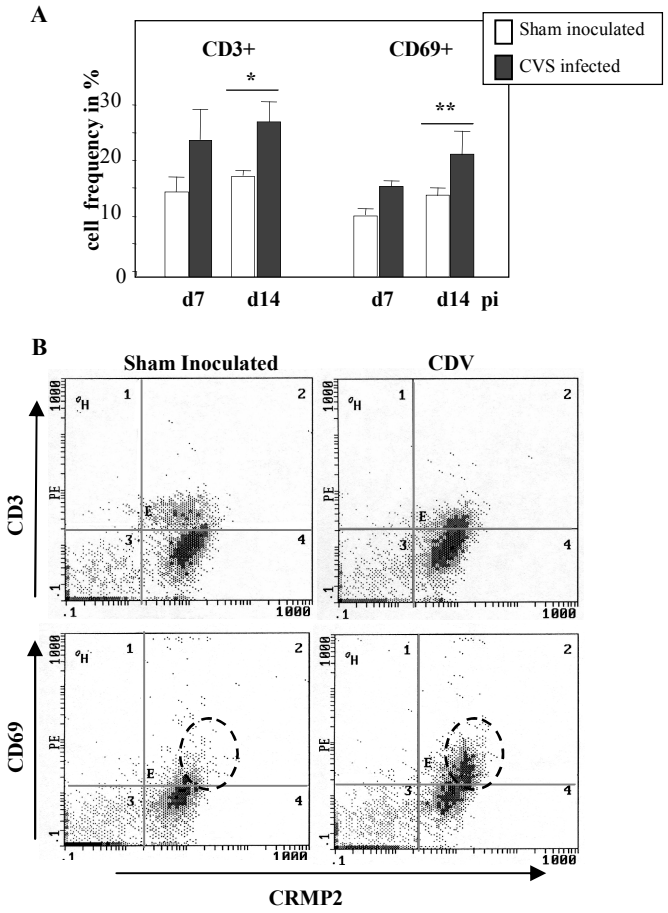

Figure-4 , Vuaillat et al

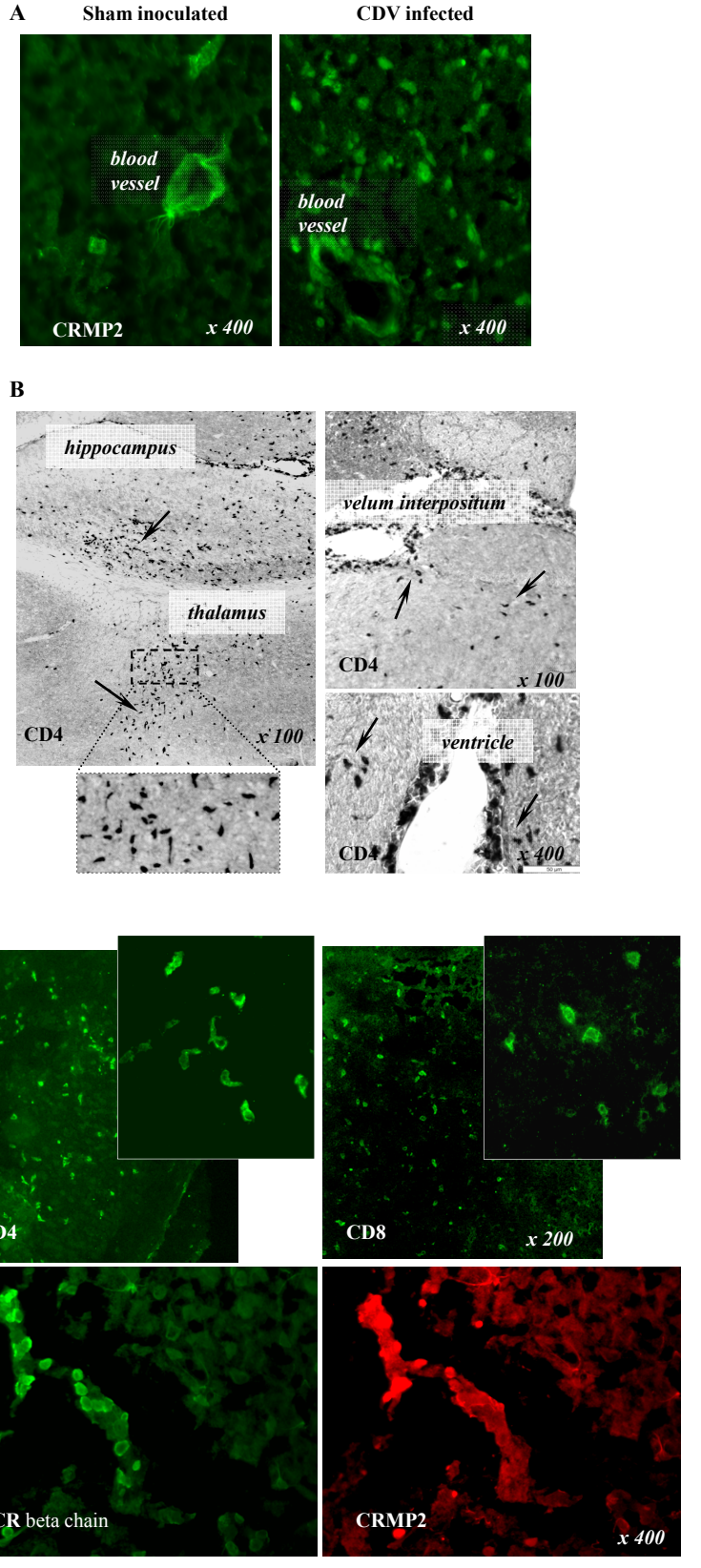

Figure-5 , Vuaillat et al

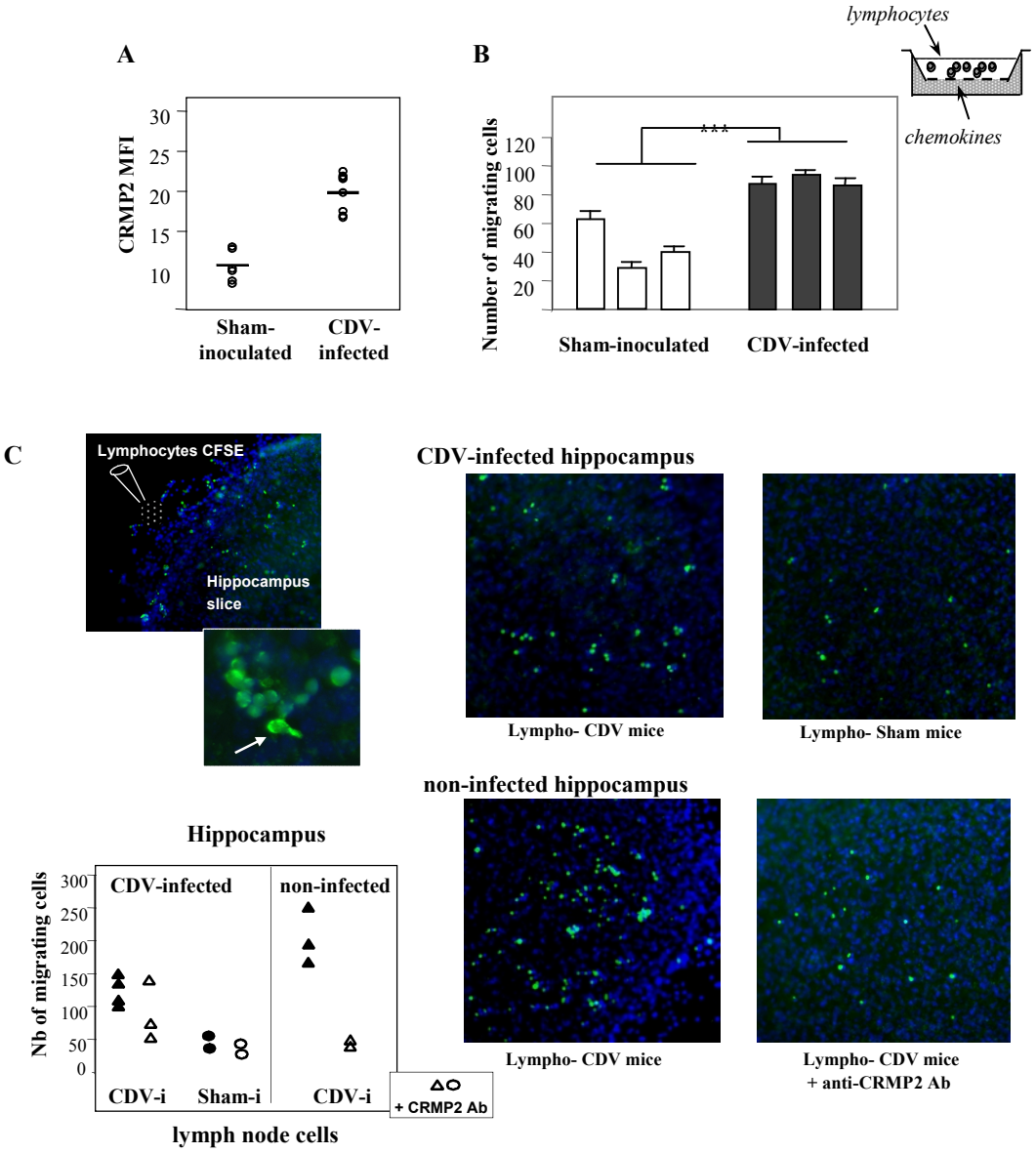

Figure-6 , Vuaillat et al

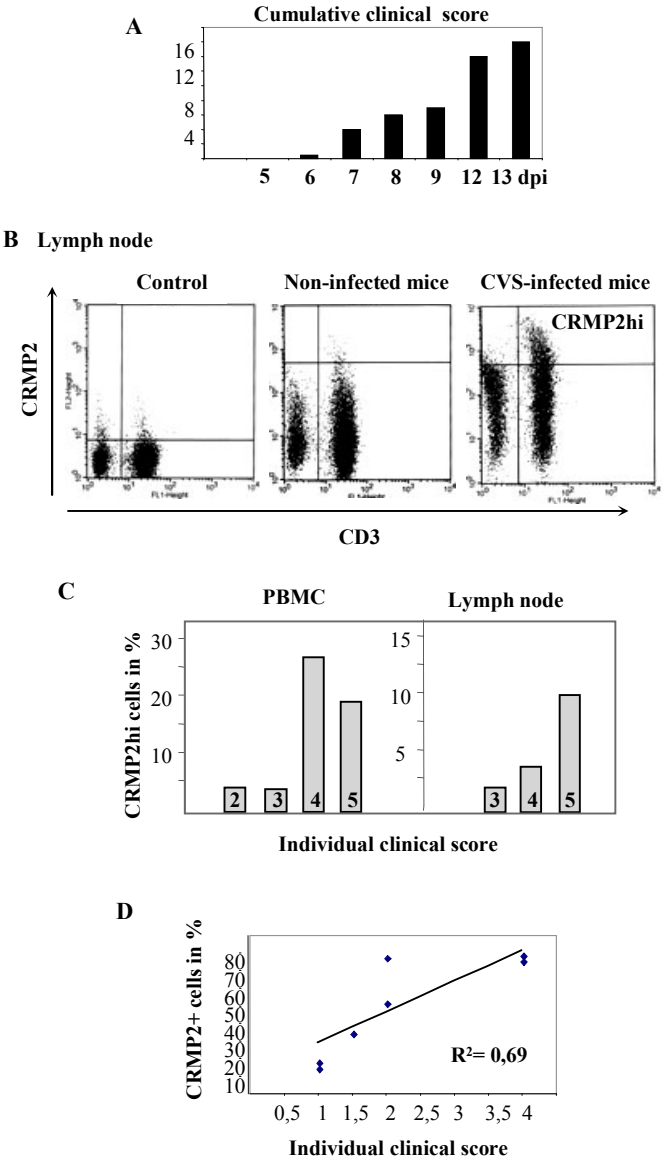

Figure-7 , Vuaillat et al